Damage-less Wet Etching for Normally-off AlGaN/GaN HEMTs Using Photo-electrochemical Reactions

Taketomo Sato, Keisuke Uemura, and Masachika Toguchi

Research Center for Integrated Quantum Electronics, Hokkaido University,
North 13, West 8, Kita-ku, Sapporo 060-0813, Japan
+81-11-706-7171, taketomo@rciqe.hokudai.ac.jp

Keywords: AlGaN/GaN, HEMTs, wet etching, photo-electrochemical reactions, low damage

Abstract

This paper describes our recent efforts to optimize photo-electrochemical (PEC) etching for fabricating recessed-gate AlGaN/GaN high-electron-mobility transistors (HEMTs). Selecting proper light wavelength and voltage conditions enabled PEC etching on AlGaN/GaN hetero-structures to produce smooth and flat surfaces. Self-termination phenomena observed under the optimal PEC condition were useful for precisely controlling the etching depth in the AlGaN layer. A recessed-gate AlGaN/GaN HEMT fabricated with PEC etching showed positive threshold voltage and better current transport controllability than that of planar-gate and dry-etched-gate AlGaN/GaN HEMTs.

INTRODUCTION

AlGaN/GaN high-electron-mobility transistors (HEMTs) are promising devices to attain both high-power and high-speed switching operations for use in next-generation power electronic circuits [1-3]. One promising approach to achieve normally-off operation is adopting a recessed-gate structure [4-6], which can be fabricated by thinning the AlGaN layer beneath the gate electrode. This dry etching process is commonly used for thinning AlGaN layers, in which the etching is performed by applying plasma of an appropriate gas mixture containing a chemically reactive element. However, dry-etched surfaces tend to be negatively affected by various types of damage due to the bombardment of reactive ions and radicals [7-9].

An alternative approach is a wet-etching process utilizing a liquid-phase etchant. Wet chemical etching has been widely used for various semiconductors in view of its low-damage process. However, it is not easy to apply this technique to AlGaN and GaN due to the high chemical stability of nitride semiconductors. Especially, the chemical resistance of Ga-polar surface is so high that the high temperature etchant over 200 ˚C or molten salt (e.g. KOH) is required [10,11]. In 1996, Minsky et al. reported that the GaN surface was etched by a photoelectrochemical (PEC) reaction at room temperature in HCl and KOH aqueous solution under illumination [12]. Youtsey et al. reported that the smooth surface was obtained by the PEC etching under the diffusion-limited condition, in which the reaction rate is limited by the rate of transport of the reactants from the bulk of solution to the n-GaN surface [13]. Up to the present, various type of the photochemical and PEC etching has been developed for GaN [14-23] and AlGaN [24-26] with growing a concern in the damage-less etching.

In the work we report in this paper, we focused on our recent study on the low-damage wet-etching for GaN and AlGaN surfaces using a PEC reaction [26,27]. Our PEC etching, which is conducted using the pulsed bias, is a cyclic process consisting of anodic oxidation and subsequent dissolution of the resulting oxide in an electrolyte. By tuning the PEC conditions such as anodic voltage and illumination, we were able to precisely control V_{th} and improve current transport controllability in recessed-gate AlGaN/GaN HEMTs.

BASIC PRINCIPLE OF PEC ETCHING

Typically, wet chemically etching III-V compounds involves the use of an oxidant to oxidize the surface, followed by dissoluting its oxide into a pH-controlled solution. For PEC etching, the surface was etched by repeating the anodic oxidation and its dissolution into the electrolyte, as schematically shown in Fig 1(a). By applying the anodic bias in the electrolyte, the AlGaN surface was oxidized as

$$\mathrm{AlGaN} + 6\,\mathrm{OH^-} + 6\,\mathrm{h^+} \rightarrow 1/2\,\mathrm{Al_2O_3} + 1/2\,\mathrm{Ga_2O_3} + 3\,\mathrm{H_2O} + 1/2\,\mathrm{N_2} \quad (1)$$

The Al_2O_3 and Ga_2O_3 are immediately dissolved into the alkali or acid solution.

Figure 1(b) schematically shows the potential distribution of the electrolyte/AlGaN/GaN structure. In the nature of the AlGaN/GaN hetero-interface, a high electric field is induced in the AlGaN layer, resulting in the generation of high-density 2DEG. Under light of λ = 300 nm, which is absorbed in both AlGaN and GaN layers, photo-electrons and holes were transferred by the internal electric field to the 2DEG and electrolyte/AlGaN interface, respectively. Accordingly, oxidation current flowed even at relatively low bias. Here, photo-carries generated in the GaN layer cannot flow due to the existence of the 2DEG and the potential barrier at the AlGaN/GaN interface. Under light of λ = 360 nm (not shown

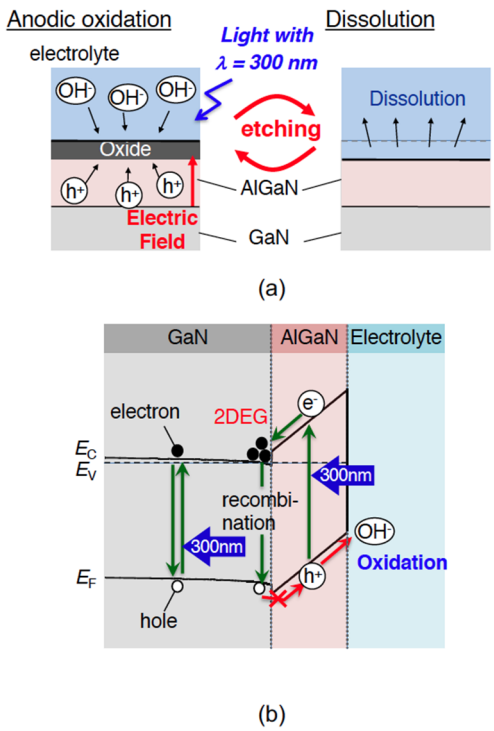

Fig. 1. Schematics of (a) the PEC etching principle and (b) the potential distribution of electrolyte/AlGaN/GaN structure.

here), which penetrates the AlGaN layer and is absorbed in the GaN layer, oxidation current was observed under the larger anodic bias. This is because the amount of electrons concentrated in 2DEG decreased with the increased reverse bias applied to the AlGaN/GaN heterostructure. In such a situation, photo holes can flow toward the electrolyte/AlGaN interface and cause oxidation reactions. Thus, we can regulate the supply of photo holes by selecting the appropriate λ and the anodic bias.

EXPERIMENTAL SETUP

For the PEC etching of AlGaN/GaN heterostructures, we used the standard electrochemical cell, which consisted of the sample to be etched as the working electrode (WE), Pt counter electrode (CE), and Ag/AgCl reference electrode (RE), as shown in Fig. 2(a). To remove the anodic oxide formed on the sample surface, we used a mixture of 1 mol/L H_2SO_4 and 1 mol/L H_3PO_4 as the electrolyte. As previously mentioned, the anodic bias and light wavelength are very important to regulate the supply of photo holes. In this study, we irradiated a monochromatic light passing through band-path filters from the top of the sample using a Xenon (Xe) lamp as the light source. The power intensity of light, P_{IN}, was adjusted using a Newport power meter (Model 843-R). Furthermore, the potential of WE with respect to RE was precisely controlled by using a potentiostat with a Princeton Applied Research Versa STAT 4. In this study, we applied the etching bias (V_{EC})

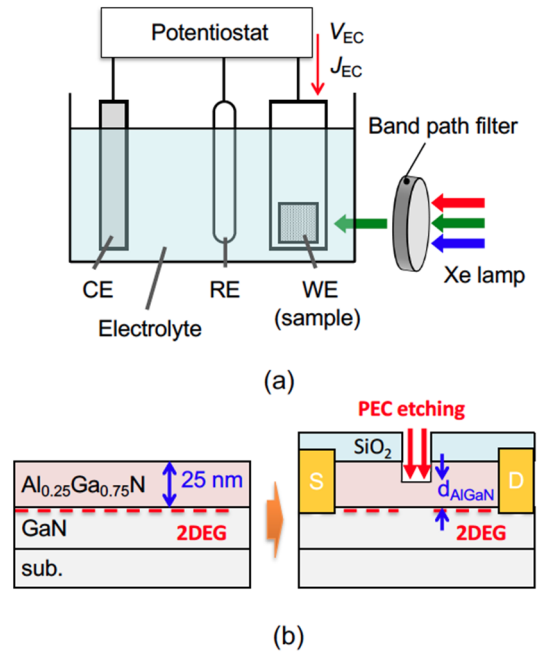

Fig. 2. Schematics of (a) the PEC etching setup and (b) the sample preparation for the AlGaN/GaN HEMTs.

in the pulsed mode to obtain a smooth and flat surface after the PEC etching. The timing of the etching stop was determined by monitoring the transient of the etching current density (J_{EC}).

An i-$Al_{0.25}Ga_{0.75}N$/i-GaN hetero-structure grown on a Si or SiC substrate was used as the starting wafer, as shown in Fig. 2(b). The initial thickness of the AlGaN barrier layer was 25 nm. A Ti/Al/Ti/Au (20/50/20/50 nm) multilayer ohmic electrode was formed using the electron-beam evaporation method, followed by annealing at 800°C for 1 min in N_2 ambient. Then, a SiO_2 film (100 nm) was formed by sputtering and lithography to define the etching region. The AlGaN/GaN sample was set on a Teflon holder and the ohmic electrodes were connected to the outer circuit via the embedded wires. The oxidation currents were supplied via the 2DEG channel, in which the open region was selectively reacted with the electrolyte. Here, the key point is how we can control the AlGaN layer (d_{AlGaN}) thickness beneath the gate electrode. Before device fabrication, we investigated the basic properties of the PEC etching by changing the anodic bias and light wavelength in terms of the photo-carrier regulation. After optimizing the PEC condition, we fabricated Schottky-gate HEMTs and MIS-gate HEMTs to evaluate the effect of the PEC etching on the electrical properties of the AlGaN/GaN hetero-structures. For the latter, we deposited an Al_2O_3 film with a nominal 30 nm thickness onto the AlGaN surface using an atomic layer deposition (ALD) system (SUGA-SAL1500) at 300° C. Then, we conducted a post-deposition-annealing (PDA) at 400° C in N_2 ambient to improve the Al_2O_3 film quality and/or the Al_2O_3/AlGaN interface.

BASIC PEC-ETCHING PROPERTIES ON ALGAN/GAN HETERO-STRUCTURES

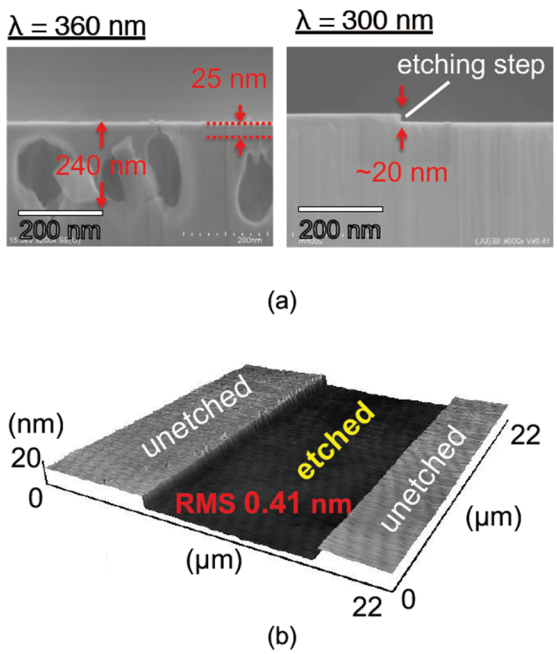

Fig. 3. Cross-sectional SEM images of samples after the PEC etching with (a) $\lambda = 360$ nm and (b) $\lambda = 300$ nm. (c) AFM image of the PEC etched sample with $\lambda = 300$ nm.

We first carried out the PEC etching on AlGaN/GaN hetero-structure samples by comparing two kinds of illumination with different wavelengths. Figures 3(a) and (b) show respectively the cross-sectional SEM images of the samples after the PEC etching with $\lambda = 360$ nm and $\lambda = 300$ nm. Small pores about 100 nm in diameter were observed in the sample formed with $\lambda = 360$ nm, where the pore etching depth of about 250 nm penetrated through the top AlGaN layer. As shown in Fig. 3(a), the pore diameter in the GaN layer increased with the etching time but that in the AlGaN layer remained unchanged. This indicates that carrier transfer occurred at the electrolyte/GaN interface rather than at the electrolyte/AlGaN interface, since the photocarriers were generated only in the GaN layer under illumination with $\lambda = 360$ nm. This kind of etching feature is obviously unsuitable for application to recessed-gate AlGaN/GaN HEMTs. On the other hand, we were able to clearly observe the etched step between the masked and un-masked regions after the PEC etching with $\lambda = 300$ nm, as shown in Fig. 3(b). There seemed to be no irregularity and no pore formation was seen in the sample etched by photo holes generated in the GaN layer. Figure 3(c) shows an AFM image of a sample after PEC etching with $\lambda = 300$ nm, $P_{IN} = 1.0$ mW/cm^2, and $V_{EC} = -0.2$ V. An overall flat surface was obtained in the etched region, in which the root mean square (RMS) roughness was only 0.41 nm. These results indicate that the PEC etching on AlGaN/GaN hetero-structures is more preferably conducted by the photo holes generated in the AlGaN layer under illumination with $\lambda = 300$ nm.

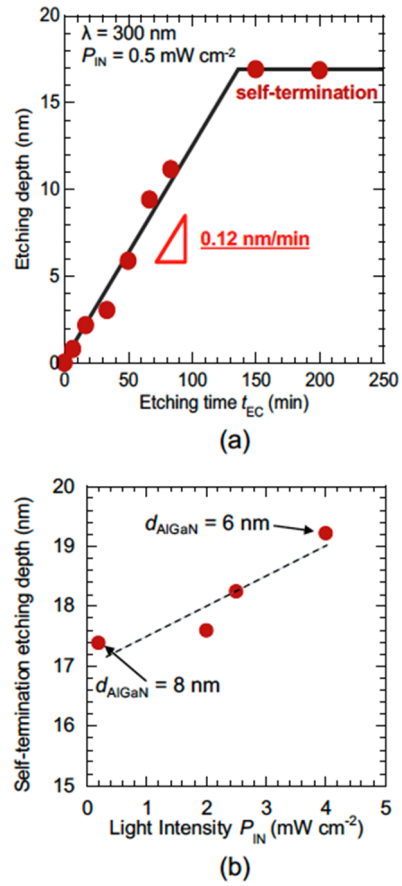

Fig. 4. (a) Relationship between etching depth and etching time and (b) relationship between self-termination depth and P_{IN}.

Figure 4(a) shows the relationship between etching depth and time obtained on the sample etched with $\lambda = 300$ nm and $P_{IN} = 0.5$ mW/cm^2. Etching depth increased linearly with etching time at the initial stage. However, the etching did not proceed more than a specific depth below the initial 25 nm AlGaN-layer thickness. Figure 4(b) shows the relationship between self-termination depth and P_{IN}. We found that the self-termination depth increased with P_{IN}, indicating this phenomenon is related to the amount of photo holes generated in the AlGaN layer. As previously mentioned, photo holes generated in the AlGaN layer are transferred to the electrolyte/AlGaN interface by an internal electric field. They cause oxidation reactions of AlGaN, and the resulting oxides dissolve in the electrolyte. Since photo holes generated in the AlGaN layer decrease due to the thinning of the layer, etching reactions are suppressed at a specific AlGaN-layer thickness, which cannot generate sufficient photo holes for surface oxidation. The AlGaN layer thinning also leads to the depletion of the 2DEG channel; thus, self-termination

phenomenon occurred. The self-termination phenomenon may help in suppressing unintentional variations in recess depth.

ELECTRICAL PROPERTIES OF RECESSED-GATE ALGAN/GAN HEMTS

On the basis of the knowledge we obtained that was described in the previous section, we fabricated AlGaN/GaN HEMTs having a recessed-gate structure by utilizing the optimal PEC condition. Figure 5(a) shows drain current-voltage (I_D-V_D) characteristics of AlGaN/GaN Schottky HEMTs having a recessed-gate structure with 10 μm gate length (L_G) and 6 nm d_{AlGaN}. The sample showed good *I-V* behavior with constant saturation currents, pinch-off characteristics and enhancement-mode operation with a positive V_{th}. Figure 5(b) shows the correlation between the V_{th} and d_{AlGaN} of AlGaN/GaN Schottky HEMTs, in which the V_{th} was defined as gate voltage (V_G) corresponding to $I_D = 10^{-6}$ A/mm. The V_{th} of the planar-gate HEMT with 25 nm d_{AlGaN} was –3.7 V. In the recessed-gate HEMTs, the V_{th} shifted respectively in the positive direction from –3.7 V to –0.6V and +0.2 V for the devices with 8 nm and 6 nm d_{AlGaN}.

To suppress the gate leakage currents in the deep forward-bias-regime, an insulating gate structure was adopted to the recessed-gate AlGaN/GaN HEMT. Figure 6(a) shows the I_D-V_D characteristics of the recessed-gate AlGaN/GaN MIS-HEMTs with 5 μm L_G, 8 nm d_{AlGaN} and 30 nm Al_2O_3 thickness. The device showed good *I-V* curves with constant saturation currents and pinch-off behavior at a low V_G bias. However, the V_{th} of MIS-HEMT was lower than the expected value obtained in the Schottky-HEMT, as shown in Fig. 5(b). Figure 6(b) compares the transfer characteristics of the recessed-gate AlGaN/GaN MIS-HEMTs for two kinds of devices conducted with and without the post metallization annealing (PMA) process [28]. The PMA successfully made the V_{th} shift in forward bias regime and enhanced the maximum transconductance value (g_m) from 60 to 66 mS/mm. A possible mechanism for the positive V_{th} shift and the g_m

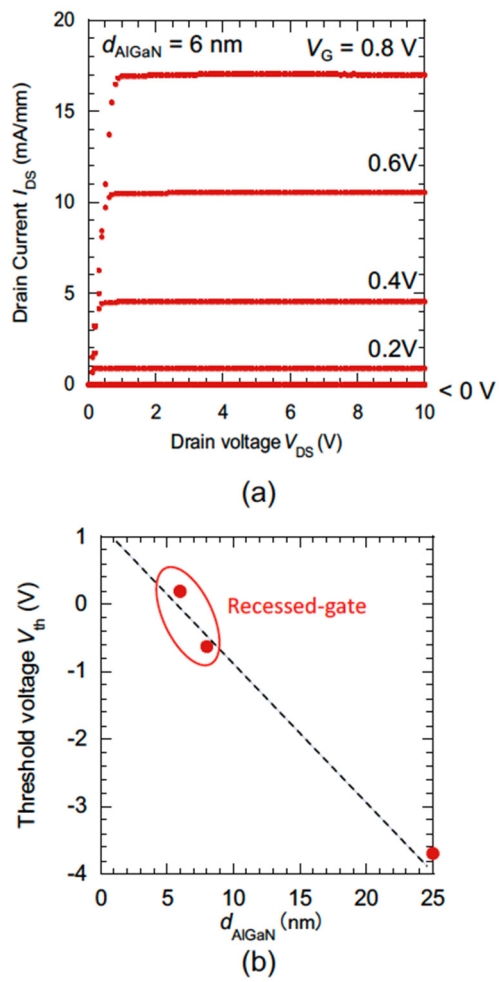

Fig. 5. (a) I_D-V_D characteristics of recessed-gate AlGaN Schottky-HEMTs with d_{AlGaN} = 6 nm and (b) relationship between V_{th} and d_{AlGaN}.

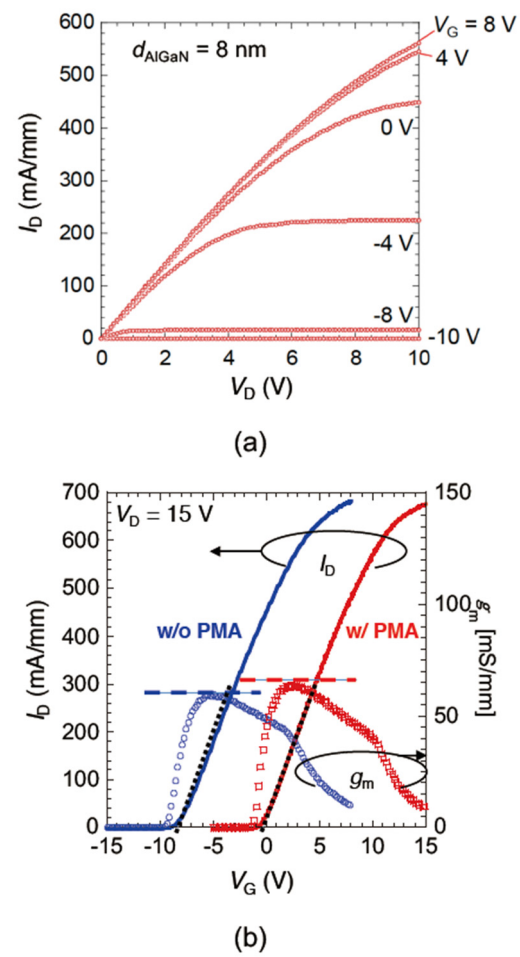

Fig. 6. (a) I_D-V_D characteristics of recessed-gate AlGaN MIS-HEMTs with d_{AlGaN} = 8 nm before PMA process and (b) comparison of their transfer characteristics before and after PMA process.

enhancement after the PMA may originate from the decrease in oxygen-related defects in the Al_2O_3/AlGaN system and subsequent shrinkage of the ALD-Al_2O_3 film caused by the relaxation of dangling bonds as reported in Ref [28-30].

Finally, we compared the electrical properties of the PEC-etched-gate devices with those of the dry-etched-gate device. The dry etching process that we employed was inductively-coupled-plasma-reactive-ion-etching (ICP-RIE), which was conducted on the AlGaN/GaN heterostructure using a BCl_3/Cl_2 gas mixture. Figure 7 shows semi-log plots of I_D-V_G and $|I_G|$-V_G characteristics measured for three kinds of devices at V_D = 15 V. We found that the $|I_G|$ was effectively reduced by the MIS-gate structure into the range of 10^{-11} A/mm, which was much smaller than that obtained in the Schottky-HEMT.

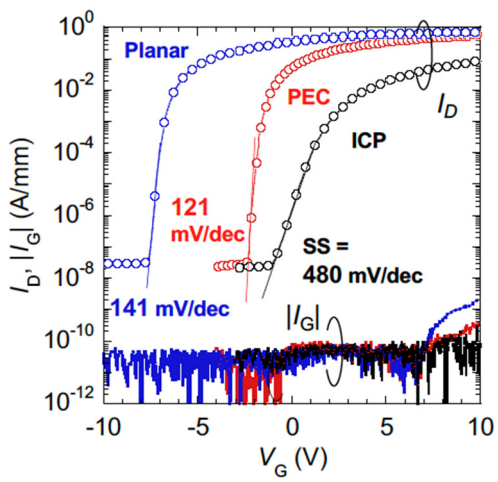

Fig. 7. Transfer characteristics of planar-gate, PEC-etched and dry-etched gate Al_2O_3/AlGaN/GaN MIS-HEMTs in the saturated region (V_{DS}=15 V).

However, there was a large difference in the sub-threshold slope (SS) obtained from the I_D-V_G characteristics. The We obtained an SS value of 141 mV/dec for the planar-gate device, whereas the dry-etched-gate device showed a much larger sub-threshold slope of 480 mV/dec. This indicates that the ICP-RIE inevitably brought plasma-related-damages to the AlGaN surfaces and/or beneath the 2DEG channel. On the other hand, the PEC-etched-gate device showed the lowest sub-threshold slope of 121 mV/dec, which indicates that the top of the AlGaN layer was etched in accordance with the nature of the low-energy electrochemical process.

Conclusion

In this paper we introduced our recent work on photo-electrochemical (PEC) etching optimized for fabricating recessed-gate AlGaN/GaN high-electron-mobility transistors (HEMTs). Photo holes generated in the AlGaN layer caused homogeneous and flat etching, in which self-termination was observed. Using light intensity enabled us to control the depth of self-termination etching; as a consequence we obtained the desired AlGaN-layer thickness. A PEC-etched Schottky-HEMT showed precisely-controlled V_{th} with AlGaN thickness, resulting in an enhanced-mode operation. The PEC-etched MIS-HEMT showed good *I-V* characteristics with constant saturation current and pinch-off behavior, and the PMA process further improved the g_m and SS values, as compared with those of planar-gate and dry-etched-gate devices. These results suggest that no significant damage was induced in the AlGaN/GaN hetero-structures during the PEC etching process. We can conclude that the PEC etching is desirable for fabricating recessed-gate structures.

Acknowledgement

This work was supported by JSPS KAKENHI Grant Numbers JP16H06421, JP17H03224.

References

[1] Y. Uemoto, M. Hikita, H. Ueno, H. Matsuo, H. Ishida, M. Yanagihara, T. Ueda, T. Tanaka, and D. Ueda, IEEE Trans. Electron Devices 54, 3393 (2007).
[2] T. Kikkawa, K. Makiyama, T. Ohki, M. Kanamura, K. Imanishi, N. Hara, and K. Joshin, Phys. Status Solidi Appl. Mater. Sci. 206, 1135 (2009).
[3] M. Kuzuhara, J. T. Asubar, and H. Tokuda, Jpn. J. Appl. Phys. 55, 070101 (2016).
[4] T. Palacios, C. S. Suh, A. Chakraborty, S. Keller, S. P. DenBaars, and U. K. Mishra, IEEE Electron Device Lett. 27, 428 (2006).
[5] S. Maroldt, C. Haupt, W. Pletschen, S. Müller, R. Quay, O. Ambacher, C. Schippel, and F. Schwierz, Jpn. J. Appl. Phys. 48, 04C083 (2009).
[6] S. Huang, X. Liu, J. Zhang, K. Wei, G. Liu, X. Wang, Y. Zheng, H. Liu, Z. Jin, C. Zhao, C. Liu, S. Liu, S. Yang, J. Zhang, Y. Hao, and K. J. Chen, IEEE Electron Device Lett. 36, 754 (2015).
[7] T. Hashizume and R. Nakasaki, Appl. Phys. Lett. 80, 4564 (2002).
[8] Z. Mouffak, A. Bensaoula, and L. Trombetta, J. Appl. Phys. 95, 727 (2004).
[9] K. Tang, W. Huang, and T. P. Chow, J. Electron. Mater. 38, 523 (2009).
[10] Y. Morimoto, J. Electrochem. Soc. 121, 1383 (1974).
[11] M. G. Mynbaeva, Electrochem. Solid-State Lett. 2, 404 (1999).
[12] M. S. Minsky, M. White, and E. L. Hu, Appl. Phys. Lett. 68, 1531 (1996).
[13] C. Youtsey, I. Adesida, L. T. Romano, and G. Bulman, Appl. Phys. Lett. 72, 560 (1998).
[14] H. Lu, Z. Wu, and I. Bhat, J. Electrochem. Soc. 144, L8 (1997).
[15] L. H. Peng, C. W. Chuang, J. K. Ho, C. N. Huang, and C. Y. Chen, Appl. Phys. Lett. 72, 939 (1998).
[16] I. M. Huygens, K. Strubbe, and W. P. Gomes, J. Electrochem. Soc. 147, 1797 (2000).

[17] C. H. Ko, Y. K. Su, S. J. Chang, W. H. Lan, J. Webb, M. C. Tu, and Y. T. Cherng, Mater. Sci. Eng. B Solid-State Mater. Adv. Technol. 96, 43 (2002).
[18] Z. H. Hwang, J. M. Hwang, H. L. Hwang, and W. H. Hung, Appl. Phys. Lett. 84, 3759 (2004).
[19] S. Lee, S. Mishkat-Ul-Masabih, J. T. Leonard, D. F. Feezell, D. A. Cohen, J. S. Speck, S. Nakamura, and S. P. DenBaars, Appl. Phys. Express 10, 011001 (2017).
[20] F. Horikiri, Y. Narita, and T. Yoshida, Jpn. J. Appl. Phys. 57, 086502 (2018).
[21] F. Horikiri, H. Ohta, N. Asai, Y. Narita, T. Yoshida, and T. Mishima, Appl. Phys. Express 11, 091001 (2018).
[22] S. Matsumoto, M. Toguchi, K. Takeda, T. Narita, and T. Kachi, Jpn. J. Appl. Phys. 57, 121001 (2018).
[23] F. Horikiri, N. Fukuhara, H. Ohta, N. Asai, Y. Narita, T. Yoshida, T. Mishima, M. Toguchi, K. Miwa, and T. Sato, accepted in Appl. Phys. Express (2019).
[24] Y. L. Chiou, L. H. Huang, and C. T. Lee, IEEE Electron Device Lett. 31, 183 (2010).
[25] Z. Zhang, S. Qin, K. Fu, G. Yu, W. Li, X. Zhang, S. Sun, L. Song, S. Li, R. Hao, Y. Fan, Q. Sun, G. Pan, Y. Cai, and B. Zhang, Appl. Phys. Express 9, 084102 (2016).
[26] Y. Kumazaki, K. Uemura, T. Sato, and T. Hashizume, J. Appl. Phys. 121, 184501 (2017).
[27] K. Uemura, M. Deki, Y. Honda, H. Amano, and T. Sato, accepted in Jpn. J. Appl. Phys. (2019).
[28] S. Kaneki, J. Ohira, S. Toiya, Z. Yatabe, J. T. Asubar, and T. Hashizume, Appl. Phys. Lett. 109, 162104 (2016).
[29] S. Ozaki, K. Makiyama, T. Ohki, N. Okamoto, S. Kaneki, K. Nishiguchi, N. Hara, and T. Hashizume, Appl. Phys. Express 10, 061001 (2017).
[30] T. Hashizume, S. Kaneki, T. Oyobiki, Y. Ando, S. Sasaki, and K. Nishiguchi, Appl. Phys. Express 11, 124102 (2018).